Received: 18 February 2021 | Revised: 9 April 2021 | Accepted: 29 April 2021

DOI: 10.1002/cne.25168

RESEARCH ARTICLE

JCN RESEARCH IN SYSTEMS NEUROSCIENCE THE JOURNAL OF COMPARATIVE NEUROLOGY WILEY

Attention differentially modulates multiunit activity in the lateral geniculate nucleus and V1 of macaque monkeys

Shraddha Shah[1] | Marc Mancarella[2] | Jacqueline R. Hembrook-Short[3] | Vanessa L. Mock[4] | Farran Briggs[1,2,4,5,6]

[1]Neuroscience Graduate Program, University of Rochester Medical Center, Rochester, New York

[2]Department of Neuroscience, University of Rochester School of Medicine, Rochester, New York

[3]Physiology and Neurobiology Department, Geisel School of Medicine at Dartmouth, Lebanon, New Hampshire

[4]Ernest J. Del Monte Institute for Neuroscience, University of Rochester School of Medicine, Rochester, New York

[5]Department of Brain and Cognitive Sciences, University of Rochester, Rochester, New York

[6]Center for Visual Science, University of Rochester, Rochester, New York

Correspondence
Farran Briggs, University of Rochester School of Medicine, 601 Elmwood Ave. Box 603, Rochester, NY 14642.
Email: farran_briggs@urmc.rochester.edu

Funding information
Albert J. Ryan Foundation; Del Monte Institute for Neuroscience (Pilot); Hitchcock Foundation; National Eye Institute, Grant/Award Numbers: EY018683, EY023165, EY025219; Office of Experimental Program to Stimulate Competitive Research, Grant/Award Number: 1632738; University of Rochester (Provost); Whitehall Foundation, Grant/Award Number: 2013-05-06

Abstract

Attention promotes the selection of behaviorally relevant sensory signals from the barrage of sensory information available. Visual attention modulates the gain of neuronal activity in all visual brain areas examined, although magnitudes of gain modulations vary across areas. For example, attention gain magnitudes in the dorsal lateral geniculate nucleus (LGN) and primary visual cortex (V1) vary tremendously across fMRI measurements in humans and electrophysiological recordings in behaving monkeys. We sought to determine whether these discrepancies are due simply to differences in species or measurement, or more nuanced properties unique to each visual brain area. We also explored whether robust and consistent attention effects, comparable to those measured in humans with fMRI, are observable in the LGN or V1 of monkeys. We measured attentional modulation of multiunit activity in the LGN and V1 of macaque monkeys engaged in a contrast change detection task requiring shifts in covert visual spatial attention. Rigorous analyses of LGN and V1 multiunit activity revealed robust and consistent attentional facilitation throughout V1, with magnitudes comparable to those observed with fMRI. Interestingly, attentional modulation in the LGN was consistently negligible. These findings demonstrate that discrepancies in attention effects are not simply due to species or measurement differences. We also examined whether attention effects correlated with the feature selectivity of recorded multiunits. Distinct relationships suggest that attentional modulation of multiunit activity depends upon the unique structure and function of visual brain areas.

KEYWORDS
lateral geniculate nucleus, multiunit activity, primary visual cortex, visual spatial attention

1 | INTRODUCTION

Attention promotes the selection of behaviorally relevant sensory information from the vast amount of sensory information available at any given moment. Attention directed toward visual stimuli overlapping the receptive fields of recorded neurons, or toward preferred stimulus features, increases visual responses of single neurons in the visual cortex (Luck et al., 1997; Moran & Desimone, 1985; Motter, 1993; Treue & Martinez-Trujillo, 1999). The magnitudes of attentional gain modulations, such as increased neuronal firing rates and enhanced BOLD signals, usually increase along the visual cortical hierarchy (Carrasco, 2011; Maunsell, 2015; O'Connor et al., 2002). However, magnitudes of attention gain modulations within a visual brain area can also vary considerably across studies. This variation is especially notable in early visual brain areas like the visual thalamus, the dorsal lateral geniculate nucleus (LGN), and the primary visual

cortex (V1). Human neuroimaging studies employing fMRI have revealed relatively robust attention effects in both the LGN and V1 (Gandhi et al., 1999; Jehee et al., 2011; Kanwisher & Wojciulik, 2000; Ling et al., 2015; Liu et al., 2007; O'Connor et al., 2002; Schneider & Kastner, 2009; Somers et al., 1999; Warren et al., 2014). In contrast, studies of single neurons in monkey LGN and V1 have generally demonstrated negligible or weak modulation by visual attention, especially in comparison to within-study recordings in higher visual cortical areas (Bender & Youakim, 2001; Buffalo et al., 2010; Luck et al., 1997; McAdams & Maunsell, 1999; McAdams & Reid, 2005; McAlonan et al., 2008; Mehta et al., 2000a; Moran & Desimone, 1985). Similarly weak or inconsistent effects of attention on local field potentials (LFPs) have also been observed in V1 of humans and monkeys, compared to more robust attentional modulations of LFPs in higher visual areas (Buffalo et al., 2011; Mock et al., 2019; Yoshor et al., 2007). Some variation in the magnitude of attention effects across studies may be attributed to the use of different attention tasks, especially if they vary in difficulty, as attention effects among V1 neurons depend on task difficulty (Chen et al., 2008). However, the relatively small shifts in attention gain magnitude due to task cannot explain the large variations observed across human neuroimaging and monkey electrophysiological studies.

There are a number of possible explanations for discrepancies in attention gain magnitudes observed in the LGN and V1 across human neuroimaging and monkey electrophysiological studies. One relatively simple explanation is that effect magnitude differences are entirely due to differences in the measurement method, for example, changes in the BOLD signal relative to changes in spike counts or voltage amplitude fluctuations among small subpopulations of neurons. If attention effects are slow, relatively weak, and require long integration times or pooling across large populations of neurons to be measurable, then fMRI will yield larger attention effects compared to single-unit electrophysiology (Boynton, 2011). In this scenario, measurements that pool across populations of neurons, like multiunit and LFP recordings, should reveal larger attention effects compared to single-unit measures. Another simple explanation for discrepancies in attention gain magnitude is that humans are more engaged in attention tasks compared to monkeys, yielding more robust attention effects throughout the brain. Human subjects may be highly motivated and can be directly instructed by experimenters. Motivation in monkeys is difficult to assess and individual monkeys' strategies in completing tasks probably vary. If discrepancies in attention gain magnitudes in the LGN and V1 across human neuroimaging and monkey electrophysiology studies are simply due to measurement or species differences, then electrophysiological recordings in monkey LGN and V1 should consistently yield relatively low attention gain magnitudes. Indeed, small attention gain magnitudes are most often reported in monkey LGN and V1 electrophysiology studies (Bender & Youakim, 2001; Buffalo et al., 2010; Luck et al., 1997; McAdams & Maunsell, 1999; McAdams & Reid, 2005; Mehta et al., 2000a; Motter, 1993; but see Cox et al., 2019; Herrero et al., 2013; Mehta et al., 2000a; van Kerkoerle et al., 2017), consistent with one or both of these simple explanations.

Alternatively, discrepancies in attention gain magnitude in the LGN and V1 across human neuroimaging and monkey electrophysiology studies could be due to more nuanced functional and/or structural properties that are unique to each brain area. Unique feedforward, feedback, and local circuitry along with unique physiological response properties and functional architecture (see for review Briggs, 2020) could generate different visual and attentional modulations in the LGN and V1. For example, attention effect magnitudes vary significantly across individual V1 neurons, dependent upon task-relevant neuronal feature tuning (Hembrook-Short et al., 2017). Multiunit measurements that pool activity across small populations of V1 neurons with overlapping feature tuning could reveal stronger attention effect magnitudes if sufficient numbers of neurons within the pool are facilitated by attention. Thus, it may be possible to evoke larger magnitude attention gain modulations in monkeys, ruling out a simple species or measurement explanation for discrepancies across human neuroimaging and monkey electrophysiology studies.

To disambiguate among these alternative explanations for differential attention effects in early visual brain areas, we studied multiunit activity in the LGN and V1 of monkeys performing a contrast change detection task requiring shifts in covert visual spatial attention. Multiunit activity reflects spiking activity of many neurons located within 100–200 μm of the recording electrode (Buchwald & Grover, 1970; Legatt et al., 1980; Supèr & Roelfsema, 2005). It is therefore an intermediate measurement between single-unit electrophysiology and LFP or fMRI BOLD signals, both of which sum over 1–4 mm of cortical volume (Berens et al., 2008; Braitenberg & Schüz, 1998; Kajikawa & Schroeder, 2011; Katzner et al., 2009). An advantage to studying multiunit activity is that it is quantified using the same metric applied to single neurons: an attention index (AI) that quantifies attentional modulation of multiunit firing rate (Luck et al., 1997), even though multiunit recordings sum activity over small populations of neurons.

We had two main objectives in this study. First, we wanted to determine whether it is possible to measure attention gain magnitudes in monkey LGN or V1 that are more comparable to those observed in human neuroimaging studies. We hypothesized that the intermediate measurement of multiunit activity may provide the best opportunity to detect robust attentional modulations in early visual brain areas of monkeys. Second, we sought to determine whether discrepancies in attention gain magnitudes across human neuroimaging and monkey electrophysiology studies are due simply to species or measurement differences, or due to more nuanced properties unique to the LGN and V1. We hypothesized that because multiunit activity sums across different functional compartments in the LGN and V1, we may observe different attention gain magnitudes across these areas, even when LGN and V1 recordings are made simultaneously in the same monkeys. Specifically, multiunit recordings in macaque LGN will capture spiking activity from neurons spanning one to three layers because each LGN layer is ~100–200 μm thick (Connolly & Van Essen, 1984). In V1, which has a columnar functional architecture with columns ~50–100 μm wide containing neurons with similar feature selectivity (Hubel & Wiesel, 1974; Ikezoe et al., 2013; Nauhaus et al., 2012), multiunit recordings will capture spiking activity from

neurons spanning one to four columns. Accordingly, multiunit recordings in the LGN and V1 aggregate signals from functionally diverse pools of neurons, giving rise to the possibility that attentional modulation of multiunit activity may differ across these early visual brain areas.

To rigorously evaluate measurements of multiunit activity in the LGN and V1, we took steps to ensure that our multiunit spike sorting method was unbiased. Specifically, we used three different thresholds for sorting multiunit spikes recorded on each electrode. This enabled examination of contributions of shared noise across pooled neurons, as well as similarity between multiunit and single-unit results reported previously (Hembrook-Short et al., 2017). We also utilized multiple statistical methods to assess whether attention effects were stable and robust across brain areas, temporal windows, and individual monkeys. We discovered that attentional modulation of multiunit firing rate was robust across all V1 layers, with positive attention gain magnitudes comparable to those reported in human neuroimaging studies. In stark contrast, attentional modulation of multiunit activity in the LGN was consistently weak. Overall, attention effects were quite stable, independent of the threshold used to define multiunits or the temporal window analyzed. Additionally, attentional modulation of V1 and LGN multiunit activity correlated with multiunit feature selectivity, although these relationships differed in the two brain areas. Together these results show that robust attentional facilitation is observable in monkey V1, but not the LGN, demonstrating that differences across human neuroimaging and monkey electrophysiology studies are not due simply to species or measurement differences. Asymmetric attention gain magnitudes in the LGN and V1 in the same monkeys performing the same task suggest that attention effects depend on the unique structural and functional properties of these early visual brain areas.

2 | MATERIALS AND METHODS

This study involves new analyses of data collected as a part of previous investigations of attentional modulation of single neurons and LFPs in the LGN and V1 (Hembrook-Short et al., 2017; Hembrook-Short et al., 2019; Mock et al., 2018; Mock et al., 2019; Sharafeldin et al., 2020). Data reported here were collected from three adult female rhesus macaques (*Macacca Mulatta*), referred to as Monkeys B, O, and E. All the procedures involving data collection from monkeys followed guidelines set forth by the National Institute of Health, and were approved by the Institutional Animal Care and Use Committees at the Geisel School of Medicine and the University of California, Davis. All animals were group housed whenever possible and light/dark cycling in the housing room was at a normal cycle of 12 h each of light/dark. Surgical preparation, chamber maintenance, electrophysiological recording setup and procedures, visual stimulation, eye tracking, attention task design, and behavioral results have been described in detail previously (Hembrook-Short et al., 2017, 2019; Mock et al., 2018, 2019). Briefly, under full surgical anesthesia and in aseptic conditions, monkeys were implanted with headposts and received small craniotomies for recording access and/or chronically implanted electrodes. Monkeys were trained to maintain central fixation and to attend to one of two identical visual stimuli. Electrophysiological recordings were made in the LGN and V1 with single microelectrodes (FHC, Bowdoin, ME; Alpha Omega, Alpharetta, GA) or multielectrode arrays (MicroProbes, Gaithersburg, BD; V-probes from Plexon Inc., Dallas, TX, RRID:SCR_018784) while monkeys performed a contrast change detection task requiring shifts in covert visual spatial attention.

2.1 | Fixation and attention tasks

Monkeys were trained to perform a simple fixation task in order to measure neuronal feature tuning and an attention task to measure attentional modulation of neuronal activity. Details of visual stimulus presentation and eye tracking setup for fixation and attention tasks have been described previously (Hembrook-Short et al., 2017, 2019; Mock et al., 2018, 2019; Sharafeldin et al., 2020).

The fixation task required monkeys to maintain fixation on a central dot while a drifting sinusoidal grating or flashed stimulus was presented on the monitor at a location overlapping the receptive fields of recorded neurons. Neuronal responses in the LGN and V1 were recorded during fixation and stimulus presentation. Gratings varied in contrast, orientation, spatial and temporal frequency, or size in steps of 10 and each presentation was repeated at least twice. The flashed stimulus was a black disk 2–4° in diameter.

The attention task was a contrast change detection task using a Posner cueing paradigm (Posner, 1980) and requiring shifts in covert visual spatial attention. All three monkeys performed a contrast change detection version of the task and one monkey (Monkey E) also performed a contrast change discrimination version of the task (Hembrook-Short et al., 2017, 2019; Mock et al., 2018, 2019). Monkeys were required to deploy covert spatial attention to a cued location corresponding to one of two identical drifting sinusoidal gratings. The drifting gratings were placed equidistant from the central fixation dot within the same visual hemifield, and the location of one of the drifting gratings overlapped the receptive fields of recorded neurons. The drifting gratings were 2–4° in diameter with a fixed temporal frequency of 4 Hz, starting contrast between 20 and 70%, and optimized to the preferred orientation and spatial frequency of the majority of recorded V1 neurons. The task was carried out in alternating blocks of trials in which monkeys attended toward the grating stimulus overlapping the receptive fields of recorded neurons in the "attend-toward" condition, or attended to the other grating stimulus placed outside the receptive field in the "attend-away" condition. The color of the fixation dot cued monkeys to allocate spatial attention toward the upper or lower grating during each block of trials. For illustrative purposes, red denotes attend-toward trials and blue denotes attend-away trials; however, various colors were used for fixation dot color cues in actual sessions (Figure 1(a)). Monkeys were required to maintain central fixation throughout the entire duration of a trial. Following fixation acquisition, there was a 0.3 s cue period during which no

gratings were displayed. The cue period was followed by a stimulus display period, during which two identical drifting gratings were displayed, lasting between 1 and 3 s (duration per trial picked randomly from a hazard function with an average of 1.7 s). At the end of the stimulus display period, the contrast of one of the gratings changed. The randomized duration of the stimulus display period ensured that the contrast change occurred at an unpredictable time in all trials. In the contrast change detection version of the task, the contrast of one of the gratings increased by 10%, and monkeys were required to detect and report the change either by releasing a joystick or pushing a button. In the contrast discrimination version of the task, the contrast of one of the gratings either increased or decreased by 1, 5, 10, or 20%, and the monkey had to report the change direction by making an eye movement to one of two answer dots. Behavioral data were analyzed from sessions in which at least 5% of trials were invalidly cued, that is, the contrast change occurred at the un-cued location. This excluded 16 of 41 sessions from behavioral analysis. Behavioral results here and in previous reports (Hembrook-Short et al., 2017; Mock et al., 2019) demonstrated that all three monkeys correctly allocated attention according to the cue and their accuracy on validly cued trials was significantly greater than on invalidly cued trials (Figure 1(b) and Table S1).

2.2 | Neuronal recording and inclusion criteria

Neuronal data from 41 sessions in which monkeys correctly completed at least 30 trials in each attention condition were analyzed for this study. Of the 41 sessions, 13 sessions were from Monkey B, 6 sessions from Monkey O, and 22 sessions from Monkey E. Single electrodes (Monkeys B, O) or multielectrode arrays (Monkey E) were inserted into retinotopically aligned, parafoveal regions of the LGN and V1 (see Figure 1(d) of Mock et al., 2019), and continuous voltage data were acquired from the LGN and across the different cortical layers in V1 using methods described previously (Hembrook-Short et al., 2017, 2019; Mock et al., 2018, 2019). Receptive field centers of LGN and V1 neurons were mapped by hand and visual stimuli (2–4° in diameter) were placed centered on V1 neuronal receptive fields, which were within <1° of the receptive field centers of simultaneously recorded LGN units. Data from V1 were assigned to appropriate laminar compartment locations (supragranular [SG]; granular, [G]; infragranular [IG]) per session based on proximity of recording electrodes to orthodromically stimulated geniculocortical recipient neurons in Layer 4C (Briggs et al., 2013) or relative to the Layer 4C/5 border determined from LFP responses to flashed stimuli (Hembrook-Short et al., 2017). Multiunit spikes were obtained for all electrode channels for all sessions through the following steps: (1) raw voltage signals were filtered with a high cutoff of 8000 Hz using a Bessel filter to generate "wideband" signals; (2) wideband signals were then high-pass filtered at 250 Hz using a Butterworth filter to remove low frequency oscillations; (3) noise artifacts, large deflections that were many times greater than the average filtered wideband signal, were removed; and (4) a threshold was set at a particular number of standard deviations above the average of the filtered wideband signal and used to identify multiunit spikes as threshold crossings. Three different threshold values were used for sorting multiunit spikes per recording contact: a low threshold, which was 1.02 ± 0.03 standard deviations above the average; a medium threshold, which was 2.06 ± 0.1 standard deviations above the average; and a high threshold, which was 2.6 ± 0.1 standard deviations above the average filtered wideband signal. Accordingly, three multiunits, corresponding to each threshold level, were sorted for each of a total of 742 electrode channels from all sessions and monkeys. Each multiunit had to pass two criteria for inclusion in further analyses: (1) evidence of a visual stimulus onset response; and (2) average spike counts per 1 ms bin reaching at least 0.5 during both attend-toward and attend-away trials. Using these criteria, 63 multiunits were excluded from the low threshold group, 70 multiunits were excluded from the medium threshold group, and 284 multiunits were excluded from the high threshold group. Numbers of multiunits per structure and per monkey included for further analyses are listed in Tables 1 and S2, respectively.

2.3 | Tuning data analysis

Analyses of multiunit tuning were performed for 336 V1 multiunits and 60 LGN multiunits sorted using the medium threshold. All tuning analyses were performed using multiunits recorded in Monkey E. Multiunit tuning responses were first plotted as responses per stimulus averaged across all repeats. Responses per stimulus were baseline-corrected by subtracting the spontaneous firing rate from each response. Tuning curves were then fit to baseline-corrected response data using Gaussian functions (orientation, size), power functions (contrast), and smoothing splines (spatial and temporal frequency). The following tuning metrics were computed per multiunit from tuning curve fits: orientation half-width at half-height (HWHH, low HWHH implies sharper orientation tuning); direction selectivity index (DSI, high DSI value corresponds to high direction selectivity) computed as the baseline-corrected difference divided by the sum of peak and null orientation responses; c50, as the contrast to evoke a half-maximal response; preferred spatial and temporal frequencies (SF, TF) corresponding to the frequency with the peak response; and surround suppression index (SSI, high SSI value corresponds to strong surround suppression) computed as the baseline-corrected difference divided by the sum of the peak response and response to the largest-grating. For all but 1 LGN multiunit, a visually evoked response ratio was computed as the maximum response during tuning tests divided by the spontaneous activity. LGN and V1 multiunits with tuning for contrast and orientation were included for analyses of relationships between tuning metrics and attentional modulation (194 V1 multiunits, 45 LGN multiunits).

2.4 | Attention data analysis and statistics

To explore attentional modulation of multiunit activity in the LGN and V1, multiunit activity during the last four complete grating cycles of the

visual stimulus prior to the contrast change (Figure 1(a), gray shaded box) was extracted for all correctly completed attention trials per session. Gratings drifted at 4 Hz; thus, the duration of the full data analysis window was 1 s. Our rationale for selecting the last four complete grating cycles per trial for the analysis window was to enable comparison across all trials in which the visual stimulus was equivalent. In other words, observed changes in multiunit activity could not be attributed to differential modulation by the visual stimulus on any given trial. Additionally, to measure dynamics of attentional modulation, the full 1-s analysis window was further subdivided into three shorter time windows corresponding to the beginning (0–0.33 s), middle (0.33–0.66 s), and end (0.66–1 s) of the full 1-s analysis window. Attentional modulation of multiunit firing rate was quantified for the full 1-s analysis window and for the beginning, middle, and end analysis windows (0.33 s each) with an AI $= (Att_{toward} - Att_{away})/(Att_{toward} + Att_{away})$ where Att_{toward} is the average firing rate on attend-toward trials and Att_{away} is the average firing rate on attend-away trials. Separate AI values were calculated for the low, medium, and high thresholded multiunits and for the full, beginning, middle, and end analysis windows. AI values were then grouped by structure and laminar compartment: LGN, SG, G, and IG. Because data displayed similar trends across monkeys (Table S2), AI values for each structure/laminar compartment group were combined across all three monkeys. Peri-stimulus time histograms (PSTHs) for individual multiunits were computed by averaging multiunit activity in 1 ms bins across all trials per attention condition per session. For illustrative purposes, red PSTHs show attend-toward trials, whereas the blue PSTHs show attend-away trials (Figure 2). PSTHs included multiunit activity before time = 0, corresponding to the cue period after fixation was acquired in addition to the data analysis window (shown as time = 0–1 s, gray boxes in Figure 2). Separate PSTHs were made per multiunit for each threshold and analysis window and were also grouped by structure and laminar compartment. Average PSTHs were then computed for all multiunits per structure and laminar compartment and data combined across all three monkeys and all sessions.

Distributions of AI values were generated for each threshold and analysis window for each grouping based on structure and laminar compartment location (Figure 3(b)). Skewness values were computed for each AI distribution to determine whether the AI distributions were symmetric around the average (AI distribution skewness values in Table S3). Bootstrapped confidence intervals (CIs) were computed for the average and median AI values separately for each group at a 99.7% confidence level (alpha = 0.003, corrected for multiple comparisons using Bonferroni correction). The bootstrapping was performed using a bias corrected and accelerated percentile method with 1000 resamples per CI calculation (using the *bootci* function in MATLAB, RRID:SCR_001622). Statistical significance was determined by evaluating whether the CI contained the null value (AI = 0). If a CI range did not contain zero, the average or median AI was considered significantly different from zero with a 99.7% confidence level (average AI values and CIs in Table 1; skewness and median AI values and CIs in Table S3). The same method was used to compute bootstrapped CIs for average AI values for each monkey individually, per analysis window and structure/laminar compartment for multiunit activity sorted using the medium threshold (average AI values and CIs for individual monkeys in Table S2). Nonparametric one-sample Kolmogorov Smirnov tests corrected for multiple comparisons using Bonferroni correction ($p < .003$) were conducted to test if AI distributions were significantly different from a probability distribution with an average of zero (average ± *SEM* AI values, and Kolmogorov–Smirnov test *p*-values in Table S4).

Relationships between attentional modulation of multiunit firing rate and multiunit tuning were examined for sessions in which both tuning and attentional modulation were computed for the same multiunits. Relationships between multiunit tuning metrics and AI values were evaluated using linear regression models (using *fitlm* and *regress* functions in MATLAB, RRID:SCR_001622). Regression model outputs: beta coefficients, coefficient *p*-values, R^2, and *F*-statistics, are reported in Table 2. In the models, AI was the dependent variable and the tuning metrics were the independent variables.

3 | RESULTS

Why attention effects in early visual brain areas, such as the LGN and V1, vary considerably across human neuroimaging and monkey electrophysiology studies remains an open question (Boynton, 2011; Kanwisher & Wojciulik, 2000). Simple explanations for this discrepancy include differences across BOLD fMRI and invasive electrophysiological measurements and/or differences in attention task motivation across humans and monkeys. More complex explanations for these discrepancies could be related to unique structural and functional properties of early visual brain areas. To disambiguate among possible explanations for discrepancies in attention effects across studies, and to explore whether robust attention effects on par with those measured using fMRI in humans are observable in monkey LGN or V1, we analyzed multiunit activity in the LGN and V1 of monkeys performing a contrast change detection task requiring shifts in visual spatial attention. This study involved new analyses of datasets utilized in prior studies of attentional modulation of single neurons and LFPs in the LGN and V1 (Hembrook-Short et al., 2017, 2019; Mock et al., 2018, 2019; Sharafeldin et al., 2020). Monkeys were trained to maintain central fixation and covertly attend to one of two identical drifting gratings displayed in the same hemifield and equidistant from the fixation dot (Figure 1(a), top). One of the gratings was placed within the receptive fields of recorded V1 and LGN neurons. Trials were run in alternating blocks in which monkeys attended toward or away from the grating overlapping recorded neuronal receptive fields according to a cue (color of the fixation dot). All trials followed the same timeline (Figure 1(a), bottom). All three monkeys were significantly more accurate at detecting a change in stimulus contrast on validly cued compared to invalidly cued trials ($p < .005$ for all three monkeys, Figure 1(b), Table S1), consistent with behavioral results reported previously (Hembrook-Short et al., 2017; Mock et al., 2019). Thus, monkeys correctly allocated covert visual spatial attention according to the cue.

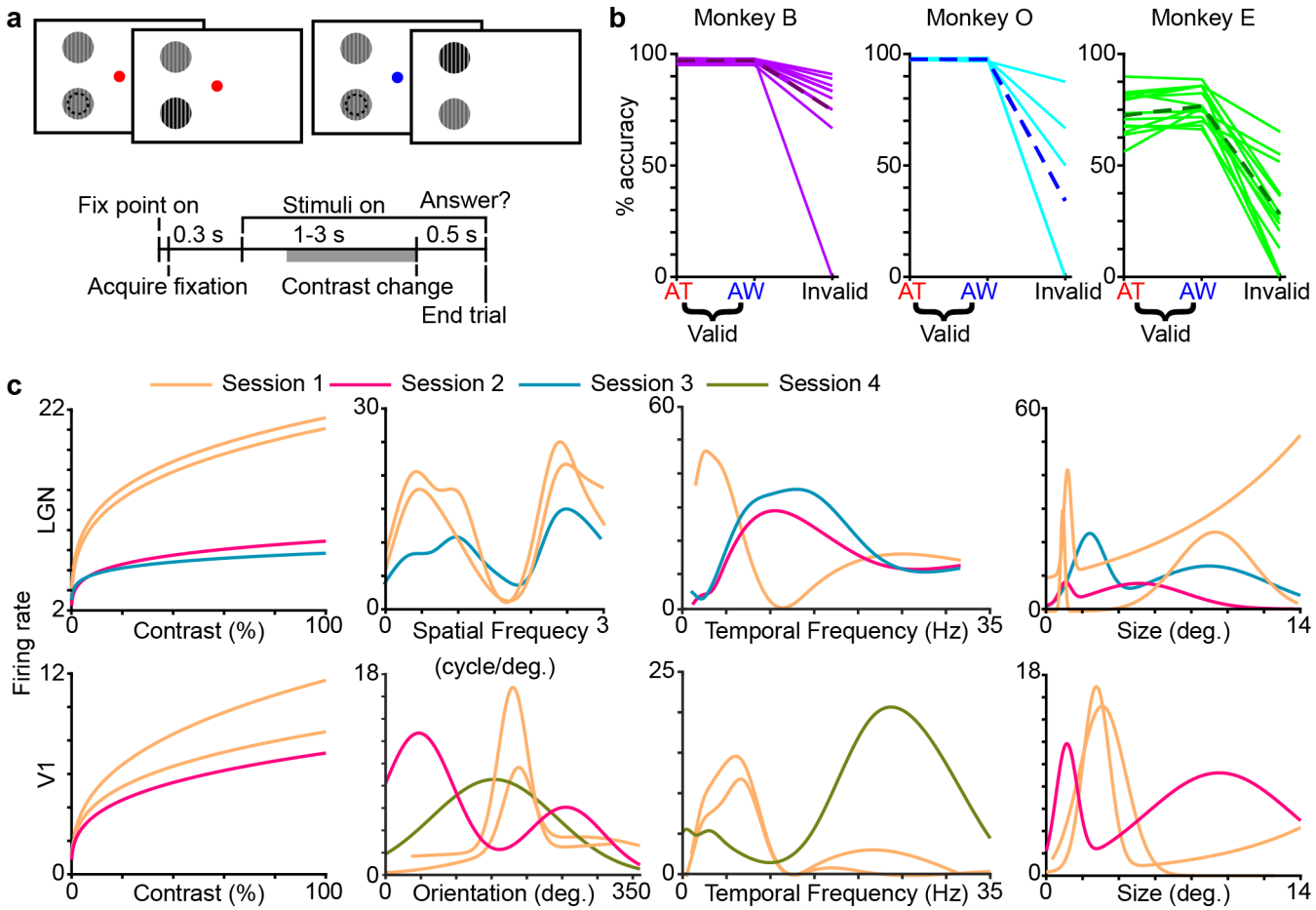

FIGURE 1 Attention task, behavioral results, and tuning for lateral geniculate nucleus (LGN) and visual cortex (V1) multiunits. (a) Schematic screenshots of attend-toward (red fixation dot) and attend-away (blue fixation dot) trials of the contrast change detection task. Dashed circle (not shown in actual task) denotes the receptive fields of recorded neurons. The timeline for a trial is shown below, with the period of trials for which data were analyzed highlighted in gray. (b) Accuracy as percent correct per session for three monkeys performing the contrast change detection task (solid lines; Monkey B: violet, Monkey O: cyan, Monkey E: green, also includes data from contrast discrimination task) for validly cued attend-toward (AT, left red label), validly cued attend-away (AW, middle blue label), and invalidly cued (Invalid, right black label) trials. Average percent correct per condition per animal is also shown (dashed lines; Monkey B: purple, Monkey O: blue, Monkey E: dark green; for statistics, see Table S1). (c) Top row: tuning curves of seven representative LGN multiunits (color-coded by recording session) in response to gratings varying in contrast, spatial frequency, temporal frequency, and size (from left to right). Bottom row: tuning curves for four representative V1 multiunits (color-coded by recording session) in response to gratings varying in contrast, orientation, temporal frequency, and size (from left to right). All firing rates are baseline-corrected [Color figure can be viewed at wileyonlinelibrary.com]

3.1 | Attentional modulation of multiunit activity in the LGN and V1

Multiunit recordings were obtained using single electrodes or multi-electrode arrays inserted into retinotopically aligned regions of the LGN and V1 (Hembrook-Short et al., 2017, 2019; Mock et al., 2018, 2019). The centers of the receptive fields of recorded LGN and V1 multiunits were highly overlapping (average distance between receptive field centers: Monkey E = 0.87 ± 0.2°; Monkey B = 0.91 ± 0.1°; Monkey O = 0.64 ± 0.1°). The full receptive fields of both LGN and V1 units were within the diameter of presented visual stimuli, which ranged from 2 to 4° in diameter and were centered over V1 receptive fields. V1 electrodes were assigned to SG, G, or IG laminar compartments. Multiunit spikes were obtained by thresholding high-pass filtered voltage data recorded on each electrode contact. Multiunits recorded in both the LGN and V1 were visually responsive and demonstrated tuning to gratings placed within their receptive fields and varying in contrast, orientation, spatial frequency, temporal frequency, and size (Figure 1(c)). A variety of tuning preferences were observed across multiunits; however, tuning for multiunits recorded in the same session was often similar, for example, V1 multiunits recorded in the same session using a linear array preferred the same orientation (Figure 1(c), orange curves).

To examine whether attentional modulation depended on multiunit sorting, three different thresholds were used to generate three multiunits per electrode contact. Thresholds were categorized as low (1.02 ± 0.03 STD), medium (2.06 ± 0.1 STD), or high (2.6 ± 0.1 STD). The number of multiunits analyzed per threshold and visual structure are

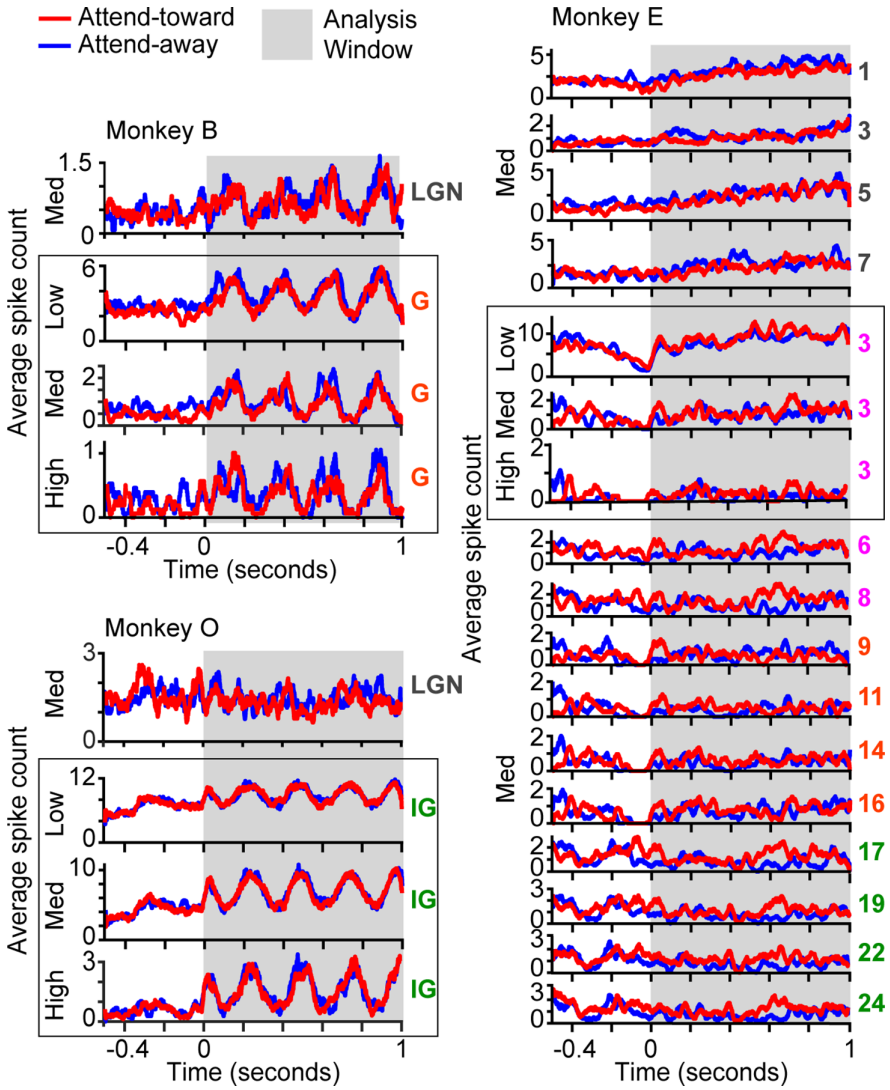

FIGURE 2 Example lateral geniculate nucleus (LGN) and visual cortex (V1) multiunit recordings from individual monkeys. Representative example average peri-stimulus time histograms (PSTHs; 1 ms bins) of multiunit activity from individual recording contacts from single sessions for each monkey (Monkey B top left, Monkey O bottom left, Monkey E right). Activity before time = 0 is during the cue period after fixation is acquired; activity between time = 0–1 (gray background) corresponds to the data analysis window. Red and blue lines are average PSTHs from attend-toward and attend-away trials, respectively. Labels at right indicate recording contact locations; LGN contacts labeled in gray, supragranular layer (SG) contacts in magenta, granular layer (G) contacts in orange, and infragranular layer (IG) contacts in green; for Monkey E, smaller numbers are more dorsal contacts. Labels at left indicate multiunit thresholding category. Boxes outline example PSTHs from an individual recording contact in V1 per monkey generated from low, medium, and high thresholded multiunits (note different *y*-axis scales). All other example PSTHs from LGN and V1 are from medium threshold multiunits [Color figure can be viewed at wileyonlinelibrary.com]

listed in Table 1. As expected, the threshold used impacted the overall firing rate of multiunits, with low thresholds generating higher firing rates and high thresholds generating lower firing rates (example multiunit PSTHs sorted using each threshold shown in boxes in Figure 2, population data per threshold shown in Figure 3(a)). Visual responses and attentional modulation appeared qualitatively consistent across multiunits generated from each threshold (Figures 2 and 3(a)). Most multiunits demonstrated changes in activity between the cue period (before time = 0) and following stimulus onset (around time = 0) and some multiunits were strongly modulated by the 4 Hz drifting grating (Figure 2). Attentional modulation varied across individual multiunits. There was evidence of both suppression (e.g., Monkey O LGN, Monkey E LGN contacts in Figure 2) and facilitation (e.g., Monkey E IG contacts in Figure 2) of multiunit firing rates with attention.

Attentional modulation of multiunits recorded in the LGN and the laminar compartments of V1, as well as across thresholds, was quantified with an AI. AI was computed as the difference divided by the sum of average firing rates in each attention condition. This created a bounded index where negative values indicate suppression with attention, positive values indicate facilitation with attention (AI = 0.33 is a doubling of firing rate with attention), and an AI value of zero indicates no effect of attention on multiunit firing rate. Initial analyses involved AI values computed for the full 1-s data analysis window and subsequent analyses involved AI values computed from shorter segments of the full analysis window, described below. Trends in AI values computed from the full 1-s data analysis window were similar across monkeys. AI values from LGN multiunits were small and suppressive in two of three monkeys; SG compartment AI values tended to be smaller than G and IG compartment AI values in all three monkeys; and IG compartment AI values demonstrated attentional facilitation in all three monkeys (Table S2(a–c)). Additionally, the ranges of AI values for each visual structure were comparable across monkeys (Table S2(a–c)). Because trends in attentional modulation were broadly consistent across the three monkeys, data were combined for subsequent population-level analyses.

Across the population, attentional modulation of multiunit activity depended more on the visual structure recorded and less on the threshold level used to obtain multiunit spikes (Figure 3). LGN multiunits did not vary across attention conditions for any threshold level, as illustrated by PSTHs of population average LGN multiunit activity

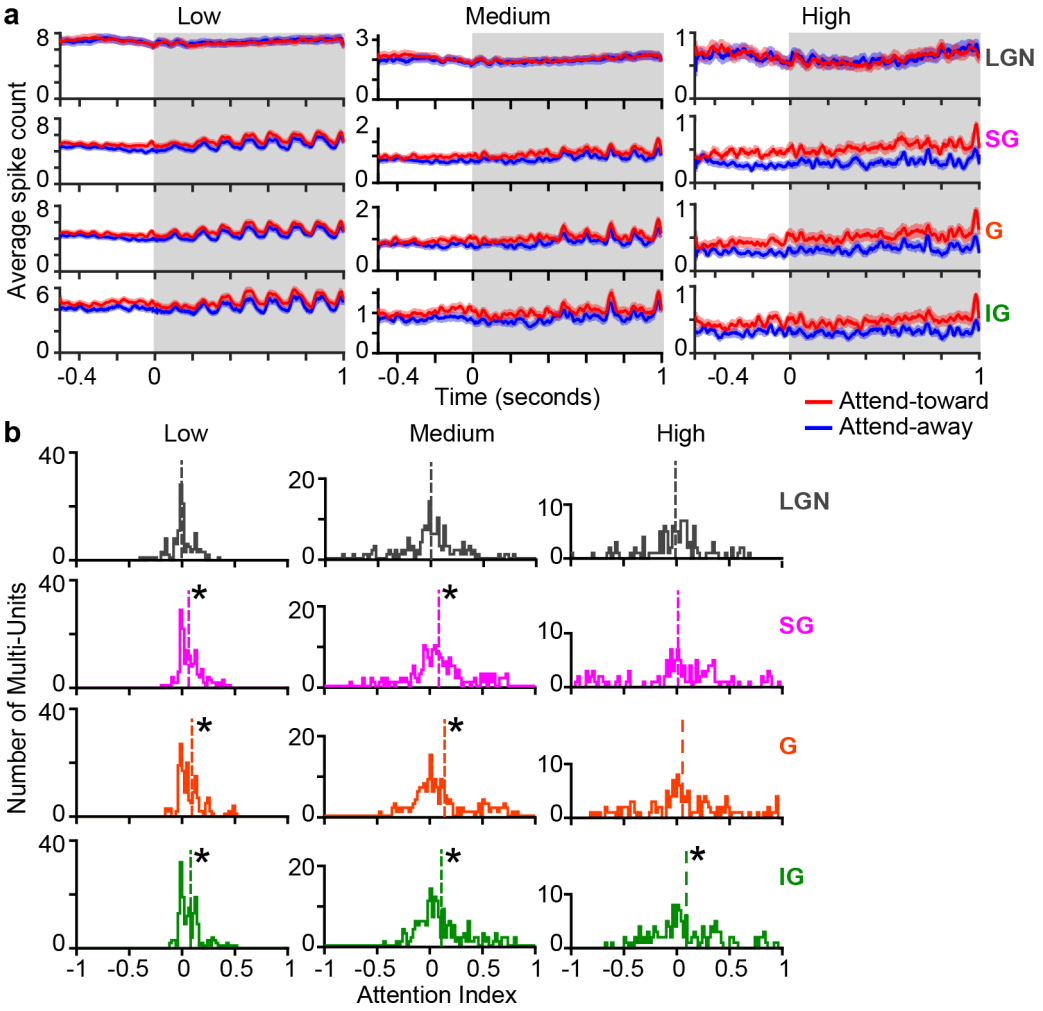

FIGURE 3 Attentional modulation of multiunit activity in the lateral geniculate nucleus (LGN) and visual cortex (V1) at different thresholds. (a) Average peri-stimulus time histograms (PSTHs) of multiunit activity recorded in the LGN (top row, gray label at right) and the supragranular (SG) (second row, magenta), granular (G) (third row, orange), and infragranular (IG) (bottom row, green) laminar compartments of V1 on attend-toward (red) and attend-away (blue) trials for low (left column), medium (middle column), and high (right column) thresholds. Red/blue shading illustrates *SEM*s; gray background illustrates data analysis window for AI calculations; time < 0 indicates the cue period (PSTH temporal conventions as in Figure 2). (b) Distributions of attention index (AI) values computed over the full 1-s trial analysis window for LGN (gray, top row), SG (magenta, second row), G (orange, third row), and IG (green, bottom row) multiunits illustrated separately for low (left column), medium (middle column) and high (right column) thresholds. Dashed colored lines illustrate distribution averages. Asterisks indicate average AI values significantly different from 0 (for statistics, see Table 1(a–c)) [Color figure can be viewed at wileyonlinelibrary.com]

(Figure 3(a), top row). Distributions of AI values for LGN multiunits at each threshold level were centered at zero (Figure 3(b), top row, gray distributions; statistics reported in Table 1(a–c), leftmost columns), suggesting that attention had no effect on the firing rates of LGN multiunits at any threshold level. Importantly, the absence of attentional modulation among LGN multiunits was not due to lack of visual responsiveness, as LGN multiunits displayed visually evoked responses greater than spontaneous activity that were uncorrelated with AI values (Figure S1).

In stark contrast to the lack of attentional modulation in the LGN, attention consistently facilitated multiunit activity in V1. For multiunits in the SG and G laminar compartments, attention significantly facilitated firing rates for low and medium thresholded multiunits (Figure 3(a,b), middle rows in magenta and orange, respectively; statistics in Table 1(a–c), middle columns). Attention consistently and significantly facilitated firing rates for multiunits in the IG laminar compartment across all thresholds (Figure 3(a,b), bottom rows in green; statistics in Table 1(a–c), rightmost columns). Thus, attentional modulation of V1 multiunits was consistently positive across layers and largely independent of threshold.

Robust attentional facilitation in V1, and no effect in the LGN, independent of threshold was clear from the averages of each AI distribution in Figure 3(b). However, distribution shapes did change depending on threshold. To further scrutinize these results, we examined the CIs for each AI distribution (Figure 4). Consistent with distribution averages showing no effect of attention, CI ranges for LGN multiunits at all thresholds overlapped the null mean, corresponding to AI = 0 (Figure 4, dashed black lines). In contrast, CI ranges for V1

TABLE 1 Average attentional modulation of multiunit activity in the LGN and V1 laminar compartments at three threshold levels with corresponding confidence interval estimations. Average AI values for the LGN and SG, G, and IG laminar compartments of V1 with low (a), medium (b), and high (c) thresholds. Data for the full 1-s trial analysis window, the beginning of the analysis window (0–0.33 s), the middle of the analysis window (0.33–0.66 s), and the end of the analysis window (0.66–1 s) are shown. Number of contacts and sessions analyzed per window and recording location are listed at the top of each table. Bootstrapped confidence intervals (99.7% confidence level, alpha = .003, corrected for multiple comparisons using Bonferroni correction) are reported for all AI distributions across visual structures and time windows. Cases in which the confidence intervals did not overlap with zero were interpreted as AIs statistically different from zero (confidence interval ranges in bold text).

(a) Low threshold: 41 sessions; 148 LGN contacts, 180 SG contacts, 182 G contacts, 185 IG contacts				
	LGN	**SG**	**G**	**IG**
Full AI (average)	−0.001	0.08	0.08	0.08
Confidence interval [lower, higher]	[−0.03, 0.03]	**[0.05, 0.1]**	**[0.05, 0.1]**	**[0.05, 0.1]**
Beginning AI (average)	−0.003	0.07	0.07	0.06
Confidence interval [lower, higher]	[−0.04, 0.03]	**[0.05, 0.1]**	**[0.04, 0.1]**	**[0.03, 0.09]**
Mid AI (average)	−0.004	0.09	0.09	0.09
Confidence interval [lower, higher]	[−0.04, 0.02]	**[0.06, 0.1]**	**[0.05, 0.1]**	**[0.06, 0.1]**
End AI (average)	0.003	0.08	0.08	0.07
Confidence interval [lower, higher]	[−0.02, 0.03]	**[0.05, 0.1]**	**[0.05, 0.1]**	**[0.05, 0.1]**
(b) Medium threshold: 41 sessions; 150 LGN contacts, 172 SG contacts, 182 G contacts, 184 IG contacts				
	LGN	**SG**	**G**	**IG**
Full AI (average)	0.0006	0.09	0.1	0.1
Confidence interval [lower, higher]	[−0.07, 0.07]	**[0.03, 0.1]**	**[0.04, 0.2]**	**[0.07, 0.2]**
Beginning AI (average)	−0.004	0.09	0.1	0.1
Confidence interval [lower, higher]	[−0.07, 0.05]	**[0.01, 0.1]**	**[0.03, 0.2]**	**[0.03, 0.2]**
Mid AI (average)	−0.02	0.09	0.09	0.1
Confidence interval [lower, higher]	[−0.08, 0.06]	**[0.02, 0.2]**	**[0.03, 0.2]**	**[0.04, 0.2]**
End AI (average)	0.02	0.08	0.1	0.09
Confidence interval [lower, higher]	[−0.05, 0.08]	**[0.02, 0.1]**	**[0.04, 0.2]**	**[0.02, 0.2]**
(c) High threshold: 33 sessions; 107 LGN contacts, 113 SG contacts, 127 G contacts, 126 IG contacts				
	LGN	**SG**	**G**	**IG**
Full AI (average)	−0.01	0.01	0.05	0.09
Confidence interval [lower, higher]	[−0.09, 0.07]	[−0.1, 0.1]	[−0.06, 0.2]	**[0.01, 0.2]**
Beginning AI (average)	−0.02	0.05	0.1	0.1
Confidence interval [lower, higher]	[−0.1, 0.06]	[−0.08, 0.2]	**[0.004, 0.2]**	**[0.05, 0.2]**
Mid AI (average)	−0.02	−0.02	−0.04	0.08
Confidence interval [lower, higher]	[−0.1, 0.08]	[−0.1, 0.1]	[−0.2, 0.06]	[−0.02, 0.2]
End AI (average)	0.03	0.03	0.05	0.08
Confidence interval [lower, higher]	[−0.05, 0.1]	[−0.09, 0.1]	[−0.04, 0.2]	[−0.02, 0.2]

Abbreviations: AI, attention index; G, granular; IG, infragranular; LGN, lateral geniculate nucleus; SG, supragranular.

multiunits sorted with low and medium thresholds were consistently above the null mean, consistent with average AI distributions showing attentional facilitation (Figure 4, left and middle). Notably, CI ranges for V1 multiunits increased with increasing threshold (Figure 4, left to right), consistent with broader AI distributions at higher thresholds among V1 multiunits (Figure 3(b)). Indeed, the variance of each AI distribution also increased across thresholds (variance for all V1 multiunits sorted at low threshold = 0.01; at medium threshold = 0.07; at high threshold = 0.12). Additionally, skewness values for AI distributions were not zero (Table S3(a–c)), suggesting that AI distributions were asymmetric. To test whether average AI values were biased by increasingly skewed AI distributions across thresholds, we estimated CIs from AI distribution medians. Median AIs and CI ranges largely matched the average values (Table S3(a–c)). Specifically, median AI results confirmed that attention did not modulate LGN multiunit activity, facilitated V1 multiunits sorted at low and medium thresholds, and did not significantly alter V1 multiunits sorted at high threshold (Table S3(a–c)). Finally, CI estimates were also broadly consistent with Kolmogorov–Smirnov significance tests of AI distribution averages (Table S4(a–c)). Overall, results of multiple statistical tests

showed that attention did not modulate firing rates of LGN multiunits sorted at any threshold and strongly facilitated firing rates among V1 multiunits sorted at low and medium thresholds and spanning all layers. Increased variance and distribution skewness for V1 multiunits sorted at high threshold generated broader CI ranges and less consistent statistical outcomes across tests.

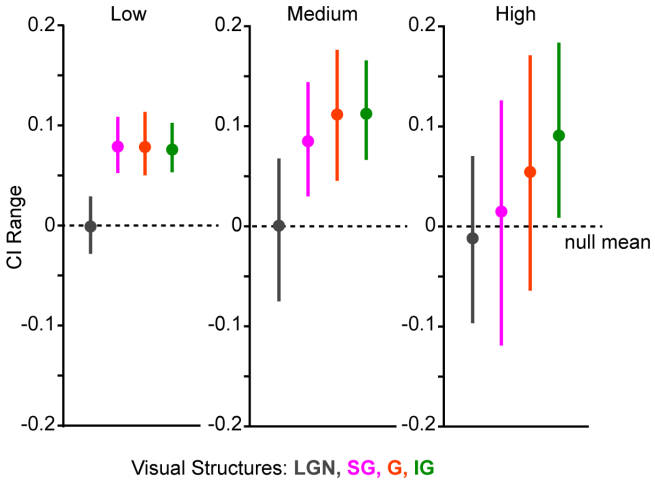

FIGURE 4 Average attention index confidence interval estimates for lateral geniculate nucleus (LGN) and visual cortex (V1) multiunits at different thresholds. Confidence interval (CI) ranges for attention index (AI) average values computed for the full 1-s analysis window. Filled circles indicate average AI values and lines indicate CI ranges for LGN (gray), supragranular (SG) (magenta), granular (G) (orange), and infragranular (IG) (green) multiunits at low (left), medium (middle), and high (right) thresholds. Dashed black line illustrates the null mean of zero. CI range units on the *y*-axis are in AI units (Figure 3(b)). Upper and lower confidence levels for each visual structure and threshold are reported in Table 1(a–c)) [Color figure can be viewed at wileyonlinelibrary.com]

3.2 | Dynamics of attentional modulation in the LGN and V1

Attention is a dynamic process (Fiebelkorn & Kastner, 2019; Ghose & Maunsell, 2002; Mock et al., 2018). To examine whether attentional modulation of multiunit firing rates varied over the time-course of trials, we subdivided the 1-s duration attention trial analysis window into three analysis windows corresponding to the beginning (0–0.33 s), middle (0.33–0.66 s), and end (0.66–1 s) of the full analysis window. These specific analysis windows were selected because behavioral and neurophysiological evidence suggest that attention fluctuates every couple hundreds of milliseconds (Fiebelkorn & Kastner, 2019). Figure 5 illustrates average PSTHs for each of these three shorter analysis windows per visual structure using multiunits thresholded at the medium level. As observed for the full analysis window, attention did not modulate LGN multiunit activity in any of the shorter windows (Figure 5, top row; Table 1(a–c), left columns). In contrast, attention facilitated firing rates for V1 multiunits sorted at low and medium thresholds for all three shorter analysis windows (Figure 5, SG, G, and IG rows; Table 1(a,b)). Interestingly, G and IG multiunits sorted at the high threshold were significantly facilitated by attention during the beginning analysis window (Table 1(c)). These trends are also illustrated in Figure 6, which shows average AIs and CI ranges for each visual structure, threshold, and analysis window.

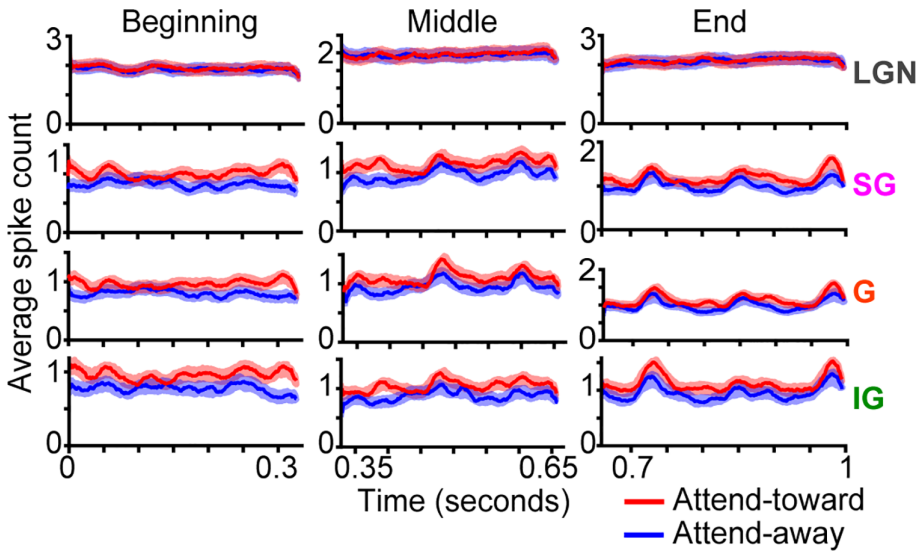

FIGURE 5 Dynamics of attentional modulation of multiunit activity in the lateral geniculate nucleus (LGN) and visual cortex (V1). Average peri-stimulus time histograms (PSTHs) of multiunit activity recorded in the LGN (top row, gray label at right) and the supragranular (SG) (second row, magenta), granular (G) (third row, orange), and infragranular (IG) (bottom row, green) laminar compartments of V1 on attend-toward (red) and attend-away (blue) trials using the medium threshold are illustrated for the beginning of the analysis window (0–0.33 s; left column), the middle of the analysis window (0.33–0.66 s; middle column), and the end of the analysis window (0.66–1 s; right column). Red/blue shading illustrates *SEM*s. Statistics are listed in Table 1(b) [Color figure can be viewed at wileyonlinelibrary.com]

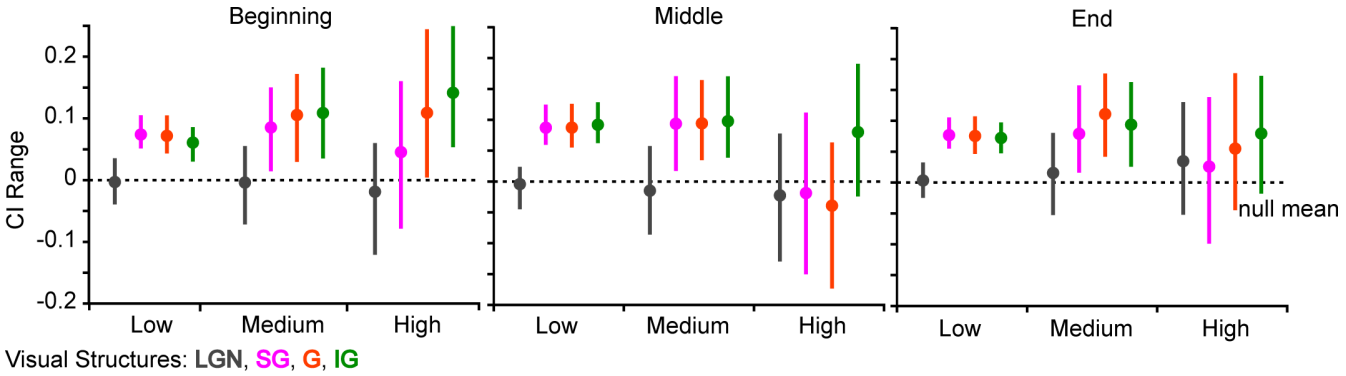

FIGURE 6 Average attention index confidence interval estimates for lateral geniculate nucleus (LGN) and visual cortex (V1) multiunits for different thresholds and analysis windows. Confidence interval (CI) ranges for attention index (AI) average values computed for three analysis windows: Beginning of the analysis window (0–0.33 s; leftmost), the middle of the analysis window (0.33–0.66 s; middle), and the end of the analysis window (0.66–1 s; rightmost). Filled circles indicate average AI values and lines indicate CI ranges for LGN multiunits (gray), supragranular (SG) multiunits (magenta), granular (G) multiunits (orange), and infragranular (IG) multiunits (green) for three threshold levels: Low threshold (left columns per panel), medium threshold (middle columns), and high threshold (right columns). Dashed black line illustrates the null mean of zero. CI range units on the *y*-axis are in AI units. Upper and lower confidence levels for each visual structure, analysis window, and threshold condition are reported in Table 1(a–c) [Color figure can be viewed at wileyonlinelibrary.com]

While attention strongly facilitated low and medium threshold V1 multiunits during all three windows, high threshold V1 multiunits only showed modest attentional facilitation during the beginning window, and this effect was not significant for all V1 multiunits. CI ranges estimated from average and median AI values computed from shorter analysis windows were mostly consistent with the following exceptions: CI ranges were not significant for median AIs for medium threshold SG multiunits during the middle window, for medium threshold G multiunits during the end window, or for high threshold G and IG multiunits during the beginning window (Table 1(a–c) and Table S3(a–c). Kolmogorov–Smirnov tests of AI distribution averages computed from shorter analysis windows were also broadly consistent with those estimated using CIs, with additional significant attentional suppression noted for low threshold LGN multiunits in some windows and significant facilitation noted for high-threshold SG multiunits in the end window (Table S4(a–c)). Together these results suggested that attentional modulation of LGN and V1 multiunits was mostly stable across the three shorter analysis windows. The only exception was the finding that significant attentional facilitation of high-thresholded V1 multiunits occurred mainly during the beginning window.

3.3 | Relationship between attentional modulation and multiunit feature selectivity

Attentional modulation of single neurons in V1 depends on the match between the feature selectivity of individual neurons and the features relevant for the task (Hembrook-Short et al., 2017). Specifically, when monkeys performed a contrast change detection task, neurons more sensitive to small changes in stimulus contrast and strongly direction selective were most facilitated by attention. We used linear regression models to evaluate possible relationships between attentional modulation and feature selectivity among LGN and V1 multiunits. We discovered a significant dependence of AI on DSI for V1 multiunits ($\beta = .45$, $p = .0009$; see Table 2 for full statistics), consistent with V1 single-unit results (Hembrook-Short et al., 2017). There was also a significant negative two-way interaction effect of c50 and DSI on AI for V1 multiunits ($\beta = -.03$, $p = .0003$; Table 2), suggesting that for multiunits with lower c50s, attentional facilitation of firing rate correlated with multiunit DSI. Although we did not observe a significant linear relationship between AI and c50 for V1 multiunits ($\beta = .008$, $p = .12$; Table 2), multiunit results were generally consistent with single-unit findings. In other words, multiunits tuned to task-relevant features, such as stimulus contrast and drift direction, were facilitated by attention. Notably, similar relationships were not observed for LGN multiunits. There was no statistical dependence of AI on c50 for LGN multiunits ($\beta = -.0007$, $p = .91$), but there was a weak relationship between preferred TF and AI for LGN multiunits ($\beta = .008$, $p = .046$). Together these findings suggest fundamentally distinct modulation of V1 and LGN multiunits by attention, with unique relationships between multiunit feature selectivity and attentional modulation of multiunit firing rate.

4 | DISCUSSION

While attentional modulation of fMRI BOLD signals in the LGN and V1 of humans can be robust, effects of attention on single neurons in the LGN and V1 of monkeys are weak (Bender & Youakim, 2001; Jehee et al., 2011; Kanwisher & Wojciulik, 2000; Luck et al., 1997; McAlonan et al., 2008; Mehta et al., 2000a; Motter, 1993; O'Connor et al., 2002; Schneider & Kastner, 2009; Warren et al., 2014). This discrepancy could be due to species: monkeys may be less motivated to perform difficult tasks and attentional modulation of V1 neurons depends on task difficulty (Chen et al., 2008). Alternatively, because

TABLE 2 Relationships between attentional modulation of firing rate and feature selectivity for LGN and V1 multiunits. Linear regression model statistics for comparisons between AI and tuning metrics (listed below) for V1 and LGN multiunits from Monkey E. Number of multiunits per comparison listed in leftmost column. Tuning metrics: Contrast to evoke a half-maximal response (c50), DSI, orientation peak HWHH, preferred SF, preferred TF, and SSI. The regression beta coefficient is considered statistically different from zero for p-values <.05 (bold text).

Regression model	Parameter	Beta coefficient	Coefficient p-value	R^2	F-statistic
V1					
AI ~ c50 + DSI + c50*DSI ($N = 194$)	c50	.008	.12		
	DSI	**.45**	**.0009**	.095	6.7
	c50*DSI	**−.03**	**.0003**		
AI ~ HWHH ($N = 194$)	HWHH	.0002	.74	.0006	0.1
AI ~ SF ($N = 185$)	SF	.005	.76	.0005	0.08
AI ~ TF ($N = 193$)	TF	.0033	.06	.02	3.5
AI ~ SSI ($N = 179$)	SSI	.0006	.95	2×10^{-5}	0.004
LGN					
AI ~ c50 ($N = 45$)	c50	−.0007	.91	.0003	0.012
AI ~ SF ($N = 44$)	SF	−.05	.19	.04	1.8
AI ~ TF ($N = 44$)	TF	**.008**	**.046**	.1	4.2
AI ~ SSI ($N = 36$)	SSI	.02	.79	.002	0.07

Abbreviations: DSI, direction selectivity index; HWHH, half-width at half-height; LGN, lateral geniculate nucleus; SF, spatial frequency; SSI, surround suppression index; TF, temporal frequency; V1, visual cortex.

BOLD signals pool across large populations of neurons and over longer timescales, weak or slow attention effect may be less visible with single neuron measures (Boynton, 2011; Logothetis, 2002; Logothetis et al., 2001). To resolve these discrepancies, we examined attentional modulation of multiunit activity, a measure of activity among small populations of neurons intermediate to single-unit, LFP, and BOLD measurements. We posited that if discrepancies between human neuroimaging and monkey electrophysiological studies are due to simple species or measurement differences, we should observe small or negligible attentional modulation of multiunit activity in both the LGN and V1. Alternatively, robust attentional modulation of multiunit activity and/or differences in attention effect magnitudes in the LGN versus V1 could suggest that attention effects depend on the unique structural or functional properties of each visual brain area. We recorded multiunit activity simultaneously in the LGN and V1 of monkeys performing attention-demanding contrast change detection tasks. We found robust attentional facilitation in all laminar compartments of V1 (Figures 3–6), with gain magnitudes comparable to those reported in human fMRI studies. V1 attention effects were consistent across analysis windows and multiunit thresholds. In stark contrast, we observed no attentional modulation of multiunit activity in the LGN for any analysis window or threshold (Figures 3–6). These results demonstrate that robust attention effects are measurable in monkey V1, thus discrepancies across prior studies are not due simply to species or measurement differences. However, markedly different attention effect magnitudes measured in the LGN and V1 of the same monkeys performing the same tasks also demonstrates that attention effects depend critically on the unique structural and functional properties of each brain area.

4.1 | Attention effects in the LGN

Surprisingly, attention consistently had no impact on the firing rates of LGN multiunits. This lack of attentional modulation cannot be explained by multiunit inactivity because LGN multiunits were nicely tuned for task-relevant stimulus features (Figure 1(c)) and were modulated by visual stimuli during tuning tests (Figure S1) and attention trials (Figure 2). Additionally, monkeys were engaged in the task (Figure 1(b)) and strong attention effect magnitudes were observed in simultaneously recorded and retinotopically aligned V1 multiunits (Figures 3–6). The absence of attentional modulation among LGN multiunits was also not due to biases in multiunit sorting methods. We found a clear lack of attentional modulation across all three multiunit sorting thresholds tested. Finally, we also considered the possibility that the magnitude of attentional effects could be obscured by averaging across the entire analysis window, given that attention is a dynamic process, and has been suggested to fluctuate at 3–8 Hz (Fiebelkorn & Kastner, 2019; Ghose & Maunsell, 2002; Mock et al., 2018). Analyses of attentional modulation in the LGN within three shorter windows confirmed the lack of significant attentional modulation of LGN multiunits for any time window.

Although our finding of no attentional modulation in the LGN appears to conflict with some prior monkey electrophysiology studies, a careful look at attentional modulation of LGN single-units reveals weak and inconsistent attention effects. Prior studies reported small effects of attention on LGN neurons: Bender & Youakim, 2001 found 2% of recorded LGN neurons had a significant F-ratio; and McAlonan et al., 2008 reported average AI values for magnocellular and parvocellular LGN neurons of 0.05 and 0.04, respectively,

corresponding to 12–15% facilitation by attention. Another study found no attentional modulation of LGN neurons (Mehta et al., 2000a). Our findings based on a larger LGN dataset assessed with multiple statistical methods are therefore broadly consistent with single-unit LGN results reported previously. Importantly though, our examination of LGN multiunit, rather than single-unit, activity provides additional insight into how attention regulates activity in the LGN. Specifically, clear differences in attention effect magnitudes across neuronal measures (single-unit and multiunit) and fMRI suggest that there are unique structural and functional properties of the LGN that limit the resolution of attention effects to measurements of larger population activity over longer timescales. Robust attentional facilitation on the order of 21–106% has been observed in the LGN of human subjects using fMRI (Ling et al., 2015; O'Connor et al., 2002; Poltoratski et al., 2017; Poltoratski et al., 2019; Schneider & Kastner, 2009). These attentional modulations of the BOLD signal are thought to be mediated by top-down corticogeniculate circuits rather than bottom-up feedforward circuits (Poltoratski et al., 2017, 2019). Indeed, this is consistent with the notion that because BOLD signals sum over longer timescales, they are more sensitive to slower top-down feedback influences (Boynton, 2011). Attentional modulation of coherent LFPs recorded in the LGN and V1 suggests that corticogeniculate feedback circuits relay attention signals from V1 to the LGN; however, attentional modulation of these signals is dynamic over the time-course of trials (Mock et al., 2018). It is therefore possible that fMRI captures these dynamics by summing activity over long timescales while neuronal spikes fail to reveal such slow dynamic signals. Finally, attention may facilitate magnocellular neurons in the LGN more than parvocellular neurons in both monkeys and humans (McAlonan et al., 2008; Schneider & Kastner, 2009; Vanduffel et al., 2000). Our multiunits may have been biased toward parvocellular LGN neurons that outnumber magnocellular LGN neurons, contributing to the lack of attentional modulation. Interestingly, we observed a significant positive correlation between preferred temporal frequency and AI among LGN multiunits (Table 2), perhaps suggesting that some multiunits preferring high temporal frequencies (e.g., with greater contributions from magnocellular neurons) were facilitated by attention, consistent with prior findings.

4.2 | Attention effects in V1

We observed average attentional modulation of multiunits across the layers of V1 on the order of a 30% facilitation of firing rate (Table 1). This is closer to the range of attention effect magnitudes observed in human neuroimaging studies compared to those observed in monkey single-unit electrophysiology studies. Attention effect magnitudes among monkey V1 single neurons vary somewhat across studies, although the majority of these report weak effects, especially in direct comparison to attention effect magnitudes measured in extrastriate visual cortex (e.g., Buffalo et al., 2010; Luck et al., 1997). Some variations in V1 attention effect magnitudes are likely attributable to tasks that may engage top-down modulations more strongly (e.g., Ito & Gilbert, 1999; Van Kerkoerle et al., 2017), or vary in difficulty (Chen et al., 2008). Other variations are likely due to laminar recording location and tuning of individual neurons to task-relevant features (Cox et al., 2019; Hembrook-Short et al., 2017; Mehta et al., 2000b; Van Kerkoerle et al., 2017). In general, average attentional facilitation of neurons in monkey V1 is typically between 0 and 15% (Buffalo et al., 2010; Luck et al., 1997; McAdams & Reid, 2005; Mehta et al., 2000a) with some individual neurons demonstrating strong facilitation or suppression (e.g., Hembrook-Short et al., 2017). Attention effect magnitudes in human V1 measured with fMRI are much larger: on the order of 50–100% facilitation (Gandhi et al., 1999; Jehee et al., 2011; Kamitani & Tong, 2005; Kanwisher & Wojciulik, 2000; Liu et al., 2007; Poltoratski et al., 2017; Saenz et al., 2002; Somers et al., 1999; Warren et al., 2014).

Attentional modulation of V1 multiunit activity was surprisingly consistent across layers and time windows and was independent of the threshold used to define multiunits, suggesting that these attention effects were robust. Attentional facilitation of IG multiunits was similar in magnitude for all thresholds and most time windows. Attentional facilitation of SG and G multiunits was similar for low and medium thresholds for all time windows (Figures 4 and 6). Robust facilitation of IG multiunits is consistent with previous findings showing that neurons in the IG layers were often more strongly facilitated by attention in comparison to relatively weak attentional modulation in the G layers (Cox et al., 2019; Hembrook-Short et al., 2017; Self et al., 2013; Van Kerkoerle et al., 2017). Some prior studies noted stronger attention effects among SG neurons compared to those we report (Cox et al., 2019; Self et al., 2013; Van Kerkoerle et al., 2017), but this could be due to task and stimulus differences. We also observed subtle dynamics in attentional modulation of high thresholded G and IG multiunits. Specifically, G and IG high threshold multiunits were facilitated by attention during the beginning of the trial, but not during the middle or end trial windows (Figure 6). These temporal dynamics of attentional facilitation are consistent with our knowledge of local circuits and thalamo-cortico-thalamic connections. Neurons in the G and IG laminar compartments receive direct LGN inputs, and are also strongly interconnected with each other (Briggs & Callaway, 2001; Briggs & Usrey, 2007). Attentional facilitation specifically at the beginning of the trial fits with previous research suggesting that attention facilitates synaptic communication between the LGN and V1 and in G-IG local circuits (Briggs et al., 2013; Hembrook-Short et al., 2019) and also facilitates corticogeniculate feedback communication with the LGN at the beginning of trials (Mock et al., 2018).

Interestingly, attentional modulation of LFPs in monkey and human V1 is as variable, if not more variable, than attentional modulation of V1 single neurons. Some groups observed no attentional modulation or suppression of V1 LFPs with attention (Chalk et al., 2010; Mock et al., 2019; Yoshor et al., 2007) while others observed facilitation of V1 LFPs with attention (Cox et al., 2019; Van Kerkoerle et al., 2017). Although some have suggested that LFP modulations are a useful proxy for the BOLD signal (Logothetis et al., 2001), this is not the case for V1. Instead, multiunit activity is a better intermediate

between single neuronal modulations and those measured with human neuroimaging. The more localized region over which multiunit measures integrate neuronal signals could in fact yield sharper and larger magnitude sensory responses compared to diffuse LFPs that integrate across larger volumes (Kajikawa & Schroeder, 2011). Thus, multiunit activity may provide a useful link between neuronal and BOLD signals. Why, though, do multiunit signals align nicely with BOLD signals in V1, but not the LGN?

4.3 | Asymmetric attention effects in the LGN and V1

One possible explanation for asymmetric attentional modulation in the LGN and V1 of monkeys is that attention tasks performed by monkeys do not engage the LGN as well as the visual cortex and other subcortical structures. Using fMRI to study attention in monkeys, Bogadhi et al. (2018) observed attentional modulation in V1 and extrastriate visual cortex as well as in the superior colliculus and pulvinar, but not in the LGN. Interestingly, stronger attentional modulation has also been reported in the human superior colliculus compared to the LGN (Schneider & Kastner, 2009). Cortical feedback to the LGN differs fundamentally from cortical connections to the superior colliculus and pulvinar in that corticogeniculate inputs are modulatory while corticocollicular and corticopulvinar inputs are driving (Sherman & Guillery, 1998). This does not explain why attentional modulation of BOLD signals in human LGN is more robust, but it does provide clues about underlying structural and functional differences between the LGN and V1 that may explain differential effects of attention.

The LGN and V1 differ in multiple important aspects: local functional architecture, feedback circuits, and the nature of visual neuronal responses and neuronal feature selectivity. The LGN is a laminar structure, and neurons within the same LGN layer are functionally homogeneous (Connolly & Van Essen, 1984). In comparison, V1 has a columnal architecture and neurons within the same vertical column have similar feature selectivity, such as orientation tuning (Gur et al., 2005; Hubel & Wiesel, 1972; Ringach et al., 2002). As multiunit activity pools from neurons across one to three LGN layers or one to four V1 columns, it captures signals from diverse pools of neurons whose feature selectivity is dictated by the underlying functional architecture of the visual area. Accordingly, differences in attentional modulation of multiunit activity across the LGN and V1 may reflect their distinct functional architectures.

Top-down feedback to the LGN is organized quite differently compared to top-down feedback to V1. The LGN receives cortical feedback primarily from V1, with some direct connections from extrastriate cortex (Briggs et al., 2016), and these modulatory excitatory feedback inputs are coupled to inhibitory input routed through the thalamic reticular nucleus (Sherman & Guillery, 2006). In contrast, V1 receives diverse excitatory cortical feedback connections from a variety of extrastriate visual cortical areas and it also receives input from the pulvinar, which has been implicated in selective attention (Markov et al., 2014; Saalmann & Kastner, 2011; Salin & Bullier, 1995; Sherman & Guillery, 2006; Shipp, 2003; Sincich & Horton, 2005; Zeki & Shipp, 1989). Broadly distributed feedback to V1 compared to restricted and modulatory feedback from lower visual areas to the LGN could explain robust attentional modulation of V1 multiunits compared to the absence of attentional modulation in the LGN.

LGN and V1 neurons also differ in the sparseness of their responses to visual stimuli. LGN neurons are less feature selective and thus are less sparse, while V1 neurons display a wider range of specific feature selectivity and are more sparse. V1 neurons with similar feature selectivity are clustered within the columnar architecture, which means that similarly sparse neurons are grouped into islands and surrounded by equally sparse neurons not tuned to the same stimulus features. Attentional modulation of V1 multiunit activity pooling across a cluster of neurons tuned to task-relevant stimulus features could serve to amplify signals from the cluster because surrounding signals would be suppressed (sparse and not tuned to the stimulus). This same clustering arrangement does not exist in the LGN, compounded with the fact that LGN neurons are less sparse. Thus, attentional modulation of LGN multiunits dilutes facilitating or suppressing responses among individual neurons rather than amplifying them.

Further support for the notion that asymmetric attentional modulation in the LGN and V1 is due to structural/functional differences across areas comes from our observations of unique relationships between attentional modulation of multiunit activity and multiunit feature tuning. Attentional modulation of single neurons in V1 and extrastriate areas depends on the match between neuronal feature tuning and the features requiring attention in the task (Cohen & Maunsell, 2011; Hembrook-Short et al., 2017; Treue & Martinez-Trujillo, 1999). We found similar relationships for multiunits in the LGN and V1, although the dependent tuning features were markedly different. In the LGN, we found a weak positive relationship between attentional modulation and a task-irrelevant feature, temporal frequency tuning (Table 2), such that LGN multiunits with higher preferred temporal frequencies were more modulated by attention. It is possible that multiunits preferring higher temporal frequencies (and showing more attentional modulation) were those units with a larger dynamic range of firing rates overall or were multiunits pooling activity from a larger proportion of magnocellular LGN neurons (see above). In contrast to the relationship for LGN multiunits, attentional modulation of V1 multiunits depended on task-relevant feature tuning, namely multiunit tuning for stimulus contrast and direction selectivity (Table 2). Similar to V1 single-units (Hembrook-Short et al., 2017), attention facilitated multiunit firing rates when multiunits had low c50 values and were more direction selective. This relationship was weaker for V1 multiunits compared to single-units, which is unsurprising given that multiunit feature tuning is less sharp compared to that of single neurons (Berens et al., 2008; Gur et al., 2005; Ringach et al., 2002; Supèr & Roelfsema, 2005). Importantly, relationships between multiunit feature tuning and attentional modulation are also consistent with feature-specific attentional modulation of distinct voxels in V1 fMRI studies in humans (Jehee et al., 2011; Liu et al., 2007; Warren et al., 2014).

Taken together, our results demonstrate compelling evidence of fundamentally distinct attentional modulation of neuronal activity in the LGN and V1. We observed no evidence of attentional modulation in the LGN, consistent with reports of weak or negligible attentional modulation in single LGN neurons in monkeys (Bender & Youakim, 2001; McAlonan et al., 2008; Mehta et al., 2000a). In contrast, we observed robust attentional facilitation in all V1 layers, in line with observations of robust attentional facilitation in human fMRI studies (Gandhi et al., 1999; Jehee et al., 2011; Kanwisher & Wojciulik, 2000; Liu et al., 2007; Somers et al., 1999; Warren et al., 2014). These distinct patterns of attentional modulation in the LGN and V1 remained consistent across different multiunit sorting thresholds and different analysis time periods. Thus, the discrepancies in attention effect magnitudes reported in monkey single-unit electrophysiology studies and human neuroimaging studies cannot be attributed to simple species or measurement differences. We propose that these discrepancies are in fact due to fundamental structural and functional differences across early visual brain areas. Notably, our results also demonstrate large differences in attention effect magnitudes across single neuron and multiunit measurements, even when taken from the same animals and recording sessions. This finding should encourage caution in equating attention effects of single neurons with those of multiunits, or any other measurement of pooled neuronal activity, as these measurements are likely to yield different effect magnitudes within and across visual brain areas.

ACKNOWLEDGMENTS

The authors thank Tanique McDonald and Makaila Banks for assistance with data analyses, Brianna Carr and Elise Bragg for expert technical assistance, and Drs Karen Moodie and Kirk Maurer for veterinary assistance. This work was funded by NIH (NEI: EY018683 and EY025219 to F. B., and EY023165 to J. R. H.-S.), NSF (EPSCoR 1632738), the Whitehall Foundation, the Hitchcock Foundation, the Del Monte Institute for Neuroscience at the University of Rochester, and a University of Rochester University Research Award. V. L. M. was supported by a Graduate Fellowship from the Albert J. Ryan Foundation.

CONFLICT OF INTEREST

The authors declare no competing financial interests.

AUTHOR CONTRIBUTIONS

Shraddha Shah and **Farran Briggs**: Designed the study. **Jacqueline R. Hembrook-Short**, **Vanessa L. Mock**, and **Farran Briggs**: Collected the data. **Shraddha Shah** and **Marc Mancarella**: Analyzed the data. **Shraddha Shah** and **Farran Briggs**: Wrote the manuscript.

PEER REVIEW

The peer review history for this article is available at https://publons.com/publon/10.1002/cne.25168.

DATA AVAILABILITY STATEMENT

Data and custom code that support the findings of this study are available from the corresponding author upon request.

ORCID

Farran Briggs https://orcid.org/0000-0002-4037-4731

REFERENCES

Bender, D. B., & Youakim, M. (2001). Effect of attentive fixation in macaque thalamus and cortex. *Journal of Neurophysiology*, *85*(1), 219–234. https://doi.org/10.1152/jn.2001.85.1.219

Berens, P., Keliris, G. A., Ecker, A. S., Logothetis, N. K., & Tolias, A. S. (2008). Comparing the feature selectivity of the gamma-band of the local field potential and the underlying spiking activity in primate visual cortex. *Frontiers in Systems Neuroscience*, *2*(JUN), 1–11. https://doi.org/10.3389/neuro.06.002.2008

Bogadhi, A. R., Bollimunta, A., Leopold, D. A., & Krauzlis, R. J. (2018). Brain regions modulated during covert visual attention in the macaque. *Scientific Reports*, *8*(1), 1–15. https://doi.org/10.1038/s41598-018-33567-9

Boynton, G. M. (2011). Spikes, BOLD, attention, and awareness: A comparison of electrophysiological and fMRI signals in V1. *Journal of Vision*, *11*(5), 1–16. https://doi.org/10.1167/11.5.12

Braitenberg, V., & Schüz, A. (1998). *Cortex: Statistics and geometry of neuronal connectivity*. Springer-Verlag Berlin Heidelberg. https://doi.org/10.1007/978-3-662-03733-1

Briggs, F. (2020). Role of feedback connections in central visual processing. *Annual Review of Vision Science*, *6*, 313–334. https://doi.org/10.1146/annurev-vision-121219-081716

Briggs, F., & Callaway, E. M. (2001). Layer-specific input to distinct cell types in layer 6 of monkey primary visual cortex. *Journal of Neuroscience*, *21*(10), 3600–3608.

Briggs, F., Kiley, C. W., Callaway, E. M., & Usrey, W. M. (2016). Morphological substrates for parallel streams of corticogeniculate feedback originating in both V1 and V2 of the macaque monkey. *Neuron*, *90*, 388–399. https://doi.org/10.1016/j.neuron.2016.02.038

Briggs, F., Mangun, G. R., & Usrey, W. M. (2013). Attention enhances synaptic efficacy and the signal-to-noise ratio in neural circuits. *Nature*, *499*(7459), 476–480. https://doi.org/10.1038/nature12276

Briggs, F., & Usrey, W. M. (2007). A fast, reciprocal pathway between the lateral geniculate nucleus and visual cortex in the macaque monkey. *Journal of Neuroscience*, *27*(20), 5431–5436. https://doi.org/10.1523/JNEUROSCI.1035-07.2007

Buchwald, J. S., & Grover, F. S. (1970). Amplitudes of background fast activity characteristic of specific brain sites. *Journal of Neurophysiology*, *33*, 148–159. https://doi.org/10.1152/jn.1970.33.1.148

Buffalo, E. A., Fries, P., Landman, R., Buschman, T. J., & Desimone, R. (2011). Laminar differences in gamma and alpha coherence in the ventral stream. *Proceedings of the National Academy of Sciences of the United States of America*, *108*(27), 11262–11267. https://doi.org/10.1073/pnas.1011284108

Buffalo, E. A., Fries, P., Landman, R., Liang, H., & Desimone, R. (2010). A backward progression of attentional effects in the ventral stream. *Proceedings of the National Academy of Sciences of the United States of America*, *107*(1), 361–365. https://doi.org/10.1073/pnas.0907658106

Carrasco, M. (2011). Visual attention: The past 25 years. *Vision Research*, *51*(13), 1484–1525. https://doi.org/10.1016/j.visres.2011.04.012

Chalk, M., Herrero, J. L., Gieselmann, M. A., Delicato, L. S., Gotthardt, S., & Thiele, A. (2010). Attention reduces stimulus-driven gamma frequency oscillations and spike field coherence in V1. *Neuron*, *66*(1), 114–125. https://doi.org/10.1016/j.neuron.2010.03.013

Chen, Y., Martinez-Conde, S., Macknik, S. L., Bereshpolova, Y., Swadlow, H. A., & Alonso, J. (2008). Task difficulty modulates the activity of specific neuronal populations in primary visual cortex. *Nature Neuroscience*, *11*(8), 974–982. https://doi.org/10.1038/nn.2147

Cohen, M. R., & Maunsell, J. H. R. (2011). Using neuronal populations to study the mechanisms underlying spatial and feature attention. *Neuron*, *70*(6), 1192–1204. https://doi.org/10.1016/j.neuron.2011.04.029

Connolly, M., & van Essen, D. (1984). The representation of the visual field in parvicellular and magnocellular layers of the lateral geniculate nucleus in the macaque monkey. *Journal of Comparative Neurology*, *226*(4), 544–564. https://doi.org/10.1002/cne.902260408

Cox, M. A., Dougherty, K., Adams, G. K., Reavis, E. A., Westerberg, J. A., Moore, B. S., Leopold, D. A., & Maier, A. (2019). Spiking suppression precedes cued attentional enhancement of neural responses in primary visual cortex. *Cerebral Cortex*, *29*(1), 77–90. https://doi.org/10.1093/cercor/bhx305

Fiebelkorn, I. C., & Kastner, S. (2019). A rhythmic theory of attention. *Trends in Cognitive Sciences*, *23*(2), 87–101. https://doi.org/10.1016/j.tics.2018.11.009

Gandhi, S. P., Heeger, D. J., & Boynton, G. M. (1999). Spatial attention affects brain activity in human primary visual cortex. *Proceedings of the National Academy of Sciences of the United States of America*, *96*(6), 3314–3319. https://doi.org/10.1073/pnas.96.6.3314

Ghose, G. M., & Maunsell, J. H. R. (2002). Attentional modulation in visual cortex depends on task timing. *Nature*, *419*, 616–620.

Gur, M., Kagan, I., & Snodderly, D. M. (2005). Orientation and direction selectivity of neurons in V1 of alert monkeys: Functional relationships and laminar distributions. *Cerebral Cortex*, *15*(8), 1207–1221. https://doi.org/10.1093/cercor/bhi003

Hembrook-Short, J. R., Mock, V. L., & Briggs, F. (2017). Attentional modulation of neuronal activity depends on neuronal feature selectivity. *Current Biology*, *27*(13), 1878–1887.e5. https://doi.org/10.1016/j.cub.2017.05.080

Hembrook-Short, J. R., Mock, V. L., Martin Usrey, W., & Briggs, F. (2019). Attention enhances the efficacy of communication in V1 local circuits. *Journal of Neuroscience*, *39*(6), 1066–1076. https://doi.org/10.1523/JNEUROSCI.2164-18.2018

Herrero, J. L., Gieselmann, M. A., Sanayei, M., & Thiele, A. (2013). Attention-induced variance and noise correlation reduction in macaque v1 is mediated by NMDA receptors. *Neuron*, *78*, 729–739. https://doi.org/10.1016/j.neuron.2013.03.029

Hubel, D. H., & Wiesel, T. N. (1972). Laminar and columnar distribution of geniculo-cortical fibers in the macaque monkey. *Journal of Comparative Neurology*, *146*(4), 421–450. https://doi.org/10.1002/cne.901460402

Hubel, D. H., & Wiesel, T. N. (1974). Sequence regularity and geometry of orientation columns in the monkey striate cortex. *Journal of Comparative Neurology*, *158*, 267–293. https://doi.org/10.1002/cne.901580304

Ikezoe, K., Mori, Y., Kitamura, K., Tamura, H., & Fujita, I. (2013). Relationship between the local structure of orientation map and the strength of orientation tuning of neurons in monkey V1: A 2-photon calcium imaging study. *Journal of Neuroscience*, *33*(42), 16818–16827. https://doi.org/10.1523/JNEUROSCI.2209-13.2013

Ito, M., & Gilbert, C. D. (1999). Attention modulates contextual influences in the primary visual cortex of alert monkeys. *Neuron*, *22*, 593–604. https://doi.org/10.1016/S0896-6273(00)80713-8

Jehee, J. F. M., Brady, D. K., & Tong, F. (2011). Attention improves encoding of task relevant features in the human visual cortex. *Journal of Neuroscience*, *31*(22), 8210–8219. https://doi.org/10.1523/JNEUROSCI.6153-09.2011

Kajikawa, Y., & Schroeder, C. E. (2011). How local is the local field potential? *Neuron*, *72*, 847–858. https://doi.org/10.1016/j.neuron.2011.09.029

Kamitani, Y., & Tong, F. (2005). Decoding the visual and subjective contents of the human brain. *Nature Neuroscience*, *8*(5), 679–685. https://doi.org/10.1038/nn1444

Kanwisher, N., & Wojciulik, E. (2000). Visual attention: Insights from brain imaging. *Nature Reviews NeuroscienceNeuroscience*, *1*(November), 1–10. https://doi.org/10.1038/35039043

Katzner, S., Nauhaus, I., Benucci, A., Bonin, V., Ringach, D. L., & Carandini, M. (2009). Local origin of field potentials in visual cortex. *Neuron*, *61*, 35–41. https://doi.org/10.1016/j.neuron.2008.11.016

Legatt, A. D., Arezzo, J., & Vaughan, H. G. (1980). Averaged multiple unit activity as an estimate of phasic changes in local neuronal activity: Effects of volume-conducted potentials. *Journal of Neuroscience Methods*, *2*, 203–217. https://doi.org/10.1016/0165-0270(80)90061-8

Ling, S., Pratte, M. S., & Tong, F. (2015). Attention alters orientation processing in the human lateral geniculate nucleus. *Nature Neuroscience*, *18*(4), 496–498. https://doi.org/10.1038/nn.3967

Liu, T., Larsson, J., & Carrasco, M. (2007). Feature-based attention modulates orientation-selective responses in human visual cortex. *Neuron*, *55*, 313–323. https://doi.org/10.1016/j.neuron.2007.06.030

Logothetis, N. K., Pauls, J., Augath, M., Trinath, T., & Oeltermann, A. (2001). Neurophysiological investigation of the basis of the fMRI signal. *Nature*, *412*, 150–157. https://doi.org/10.1038/35084005

Logothetis, N. K. (2002). The neural basis of the blood-oxygen-level-dependent functional magnetic resonance imaging signal. *Philosophical Transactions of the Royal Society B: Biological Sciences*, *357*(1424), 1003–1037. https://doi.org/10.1098/rstb.2002.1114

Luck, S. J., Chelazzi, L., Hillyard, S. A., & Desimone, R. (1997). Neural mechanisms of spatial selective attention in areas V1, V2, and V4 of macaque visual cortex. *Journal of Neurophysiology*, *77*, 24–42. https://doi.org/10.1152/jn.1997.77.1.24

Markov, N. T., Vezoli, J., Chameau, P., Falchier, A., Quilodran, R., Huissoud, C., Lamy, C., Misery, P., Giroud, P., Ullman, S., Barone, P., Dehay, C., Knoblauch, K., & Kennedy, H. (2014). Anatomy of hierarchy: Feedforward and feedback pathways in macaque visual cortex. *Journal of Comparative Neurology*, *522*, 225–259. https://doi.org/10.1002/cne.23458

Maunsell, J. H. R. (2015). Neuronal mechanisms of visual attention. *Annual Review of Vision Science*, *1*, 373–391. https://doi.org/10.1146/annurev-vision-082114-035431

McAdams, C. J., & Maunsell, J. H. (1999). Effects of attention on orientation-tuning functions of single neurons in macaque cortical area V4. *The Journal of Neuroscience*, *19*, 431–441.

McAdams, C. J., & Reid, R. C. (2005). Attention modulates the responses of simple cells in monkey primary visual cortex. *Journal of Neuroscience*, *25*(47), 11023–11033. https://doi.org/10.1523/JNEUROSCI.2904-05.2005

McAlonan, K., Cavanaugh, J., & Wurtz, R. H. (2008). Guarding the gateway to cortex with attention in visual thalamus. *Nature*, *456*, 391–394. https://doi.org/10.1038/nature07382

Mehta, A. D., Ulbert, I., & Schroeder, C. E. (2000a). Intermodal selective attention in monkeys. I: Distribution and timing of effects across visual areas. *Cerebral Cortex*, *10*, 343–358.

Mehta, A. D., Ulbert, I., & Schroeder, C. E. (2000b). Intermodal selective attention in monkeys. II: Physiological mechanisms of modulation. *Cerebral Cortex*, *10*(4), 359–370. https://doi.org/10.1093/cercor/10.4.359

Mock, V. L., Luke, K. L., Hembrook-Short, J. R., & Briggs, F. (2018). Dynamic communication of attention signals between the LGN and V1. *Journal of Neurophysiology*, *120*(4), 1625–1639. https://doi.org/10.1152/jn.00224.2018

Mock, V. L., Luke, K. L., Hembrook-Short, J. R., & Briggs, F. (2019). Phase shifts in high-beta-and low-gamma-band local field potentials predict the focus of visual spatial attention. *Journal of Neurophysiology*, *121*(3), 799–822. https://doi.org/10.1152/jn.00469.2018

Moran, J., & Desimone, R. (1985). Selective attention gates visual processing in the extrastriate cortex. *Science*, *229*(4715), 782–784. https://doi.org/10.1126/science.4023713

Motter, B. C. (1993). Focal attention produces spatially selective processing in visual cortical areas V1, V2, and V4 in the presence of competing stimuli. *Journal of Neurophysiology*, *70*(3), 909–919. https://doi.org/10.1152/jn.1993.70.3.909

Nauhaus, I., Nielsen, K. J., Disney, A. A., & Callaway, E. M. (2012). Orthogonal micro-organization of orientation and spatial frequency in primate

primary visual cortex. *Nature Neuroscience*, *15*, 1683–1690. https://doi.org/10.1038/nn.3255

O'Connor, D. H., Fukui, M. M., Pinsk, M. A., & Kastner, S. (2002). Attention modulates responses in the human lateral geniculate nucleus. *Nature Neuroscience*, *5*(11), 1203–1209. https://doi.org/10.1038/nn957

Poltoratski, S., Ling, S., McCormack, D., & Tong, F. (2017). Characterizing the effects of feature salience and top-down attention in the early visual system. *Journal of Neurophysiology*, *118*(1), 564–573. https://doi.org/10.1152/jn.00924.2016

Poltoratski, S., Maier, A., Newton, A. T., & Tong, F. (2019). Figure-ground modulation in the human lateral geniculate nucleus is distinguishable from top-down attention. *Current Biology*, *29*(12), 2051–2057.e3. https://doi.org/10.1016/j.cub.2019.04.068

Posner, M. I. (1980). Orienting of attention. *The Quarterly Journal of Experimental Psychology*, *32*(1), 3–25. https://doi.org/10.1080/00335558008248231

Ringach, D. L., Shapley, R. M., & Hawken, M. J. (2002). Orientation selectivity in macaque V1: Diversity and laminar dependence. *Journal of Neuroscience*, *22*(13), 5639–5651. https://doi.org/10.1523/jneurosci.22-13-05639.2002

Saalmann, Y. B., & Kastner, S. (2011). Cognitive and perceptual functions of the visual thalamus. *Neuron*, *71*(2), 209–223. https://doi.org/10.1016/j.neuron.2011.06.027

Saenz, M., Buracas, G. T., & Boynton, G. M. (2002). Global effects of feature-based attention in human visual cortex. *Nature Neuroscience*, *5*(7), 631–632. https://doi.org/10.1038/nn876

Salin, P. A., & Bullier, J. (1995). Corticocortical connections in the visual system: Structure and function. *Physiological Reviews*, *75*(1), 107–154. https://doi.org/10.1152/physrev.1995.75.1.107

Schneider, K. A., & Kastner, S. (2009). Effects of sustained spatial attention in the human lateral geniculate nucleus and superior colliculus. *Journal of Neuroscience*, *29*(6), 1784–1795. https://doi.org/10.1523/JNEUROSCI.4452-08.2009

Self, M. W., van Kerkoerle, T., Supèr, H., & Roelfsema, P. R. (2013). Distinct roles of the cortical layers of area V1 in figure-ground segregation. *Current Biology: CB*, *23*(21), 2121–2129. https://doi.org/10.1016/j.cub.2013.09.013

Sharafeldin, A., Mock, V. L., Meisenhelter, S., Hembrook-Short, J. R., & Briggs, F. (2020). Changes in local network activity approximated by reverse spike-triggered local field potentials predict the focus of attention. *Cerebral Cortex Communications*, *1*(1), 1–13. https://doi.org/10.1093/texcom/tgaa014

Sherman, S. M., & Guillery, R. W. (1998). On the actions that one nerve cell can have on another: Distinguishing "drivers" from "modulators.". *Proceedings of the National Academy of Sciences of the United States of America*, *95*(12), 7121–7126. https://doi.org/10.1073/pnas.95.12.7121

Sherman, S. M., & Guillery, R. W. (2006). *Exploring the thalamus and its role in cortical function*. MIT Press. https://doi.org/10.7551/mitpress/2940.001.0001

Shipp, S. (2003). The functional logic of cortico-pulvinar connections. *Philosophical Transactions of the Royal Society B: Biological Sciences*, *358*, 1605–1624. https://doi.org/10.1098/rstb.2002.1213

Sincich, L. C., & Horton, J. C. (2005). The circuitry of V1 and V2: Integration of color, form, and motion. *Annual Review of Neuroscience*, *28*, 303–326. https://doi.org/10.1146/annurev.neuro.28.061604.135731

Somers, D. C., Dale, A. M., Seiffert, A. E., & Tootell, R. B. H. (1999). Functional MRI reveals spatially specific attentional modulation in human primary visual cortex. *Proceedings of the National Academy of Sciences of the United States of America*, *96*(4), 1663–1668. https://doi.org/10.1073/pnas.96.4.1663

Supèr, H., & Roelfsema, P. R. (2005). Chronic multiunit recordings in behaving animals: Advantages and limitations. *Progress in Brain Research*, *147*(Special Issue), 263–282. https://doi.org/10.1016/S0079-6123(04)47020-4

Treue, S., & Martinez-Trujillo, J. C. (1999). Feature-based attention influences motion processing gain in macaque visual cortex. *Nature*, *399*, 575–579. https://doi.org/10.1038/21176

van Kerkoerle, T., Self, M. W., & Roelfsema, P. R. (2017). Layer-specificity in the effects of attention and working memory on activity in primary visual cortex. *Nature Communications*, *8*, 1–12. https://doi.org/10.1038/ncomms13804

Vanduffel, W., Tootell, R. B. H., & Orban, G. A. (2000). Attention-dependent suppression of metabolic activity in the early stages of the macaque visual system. *Cerebral Cortex*, *10*(2), 109–126. https://doi.org/10.1093/cercor/10.2.109

Warren, S. G., Yacoub, E., & Ghose, G. M. (2014). Featural and temporal attention selectively enhance task-appropriate representations in human primary visual cortex. *Nature Communications*, *5*, 5643. https://doi.org/10.1038/ncomms6643

Yoshor, D., Ghose, G. M., Bosking, W. H., Sun, P., & Maunsell, J. H. R. (2007). Spatial attention does not strongly modulate neuronal responses in early human visual cortex. *Journal of Neuroscience*, *27*(48), 13205–13209. https://doi.org/10.1523/JNEUROSCI.2944-07.2007

Zeki, S., & Shipp, S. (1989). Modular connections between areas V2 and V4 of macaque monkey visual cortex. *European Journal of Neuroscience*, *1*(5), 494–506. https://doi.org/10.1111/j.1460-9568.1989.tb00356.x

SUPPORTING INFORMATION

Additional supporting information may be found online in the Supporting Information section at the end of this article.

How to cite this article: Shah, S., Mancarella, M., Hembrook-Short, J. R., Mock, V. L., & Briggs, F. (2021). Attention differentially modulates multiunit activity in the lateral geniculate nucleus and V1 of macaque monkeys. *Journal of Comparative Neurology*, 1–17. https://doi.org/10.1002/cne.25168